The Plant Journal (2003) **35**, 393–404 doi: 10.1046/j.1365-313X.2003.01807.x

TECHNICAL ADVANCE

Classification and identification of *Arabidopsis* cell wall mutants using Fourier-Transform InfraRed (FT-IR) microspectroscopy

Grégory Mouille, Stéphane Robin†, Mannaïg Lecomte, Silvère Pagant and Herman Höfte*
Laboratoire de Biologie Cellulaire, INRA, Route de Saint Cyr, 78026 Versailles cedex, France

Received 18 December 2002; revised 1 April 2003; accepted 22 April 2003.
*For correspondence (fax +33 1 30 83 3099; e-mail Herman.Hofte@versailles.inra.fr).
†Present address: INA-PG (dpt OMIP)/INRA (dpt BIA), 16 rue Claude Bernard F-75231, Paris, France.

Summary

We have developed a novel procedure for the rapid classification and identification of *Arabidopsis* mutants with altered cell wall architecture based on Fourier-Transform Infrared (FT-IR) microspectroscopy. FT-IR transmission spectra were sampled from native 4-day-old dark-grown hypocotyls of 46 mutants and the wild type treated with various drugs. The Mahalanobis distance between mutants, calculated from the spectral information after compression with the Discriminant Variables Selection procedure, was used for α hierarchical cluster analysis. Despite the completely unsupervised nature of the classification procedure, we show that all mutants with cellulose defects appeared in the same cluster. In addition, mutant alleles of similar strength for several unrelated loci were also clustered, which demonstrates the sensitivity of the method to detect a wide array of cell wall defects. Comparing the cellulose-deficient cluster with the cluster that contained wild-type controls led to the identification of wave numbers that were diagnostic for altered cellulose content in the context of an intact cell wall. The results show that FT-IR spectra can be used to identify different classes of mutants and to characterize cell wall changes at a microscopic level in unknown mutants. This procedure significantly accelerates the identification and classification of cell wall mutants, which makes cell wall polysaccharides more accessible to functional genomics approaches.

Keywords: cell wall, cellulose, mutants, FT-IR microspectroscopy.

Introduction

Over the recent years, powerful techniques have been developed for the global analysis of transcripts, proteins, and small metabolites. Despite their biological importance, cell wall polysaccharides have remained refractory to such systematic approaches, mainly because of a lack of appropriate analytic techniques. Cell wall mutants are highly informative for the study of wall synthesis. Reiter *et al.* (1997) isolated a collection of mutants with altered neutral sugar composition, referred to as *mur1–12* (Table 1). The analysis of several loci led to the identification of enzymes in nucleotide–sugar interconversion pathways: MUR1 (Bonin *et al.*, 1997) and MUR4 (Burget and Reiter, 1999); and glycosyl transferases involved in xyloglucan (XG) synthesis, MUR2 (Vanzin *et al.*, 2002) and MUR3 (Lerouxel *et al.*, 2002). The study of cellulose-deficient dwarf mutants has identified several isoforms of the cellulose synthase catalytic subunit (CESA), an endo-β-1,4-glucanase KORRIGAN, a novel plasma membrane protein (Pagant *et al.*, 2002) and a Glucosidase II (RSW3) directly or indirectly required for the *in vivo* synthesis of this polymer (for a review, see Williamson *et al.*, 2001). Two complementation groups of embryo- or seedling-lethal mutants with altered protein glycosylation were also defective for cellulose synthesis (Gillmor *et al.*, 2002; Lukowitz *et al.*, 2001). A mutant with altered pectins carrying a mutation in a putative membrane-bound glycosyl transferase was also reported recently (Bouton *et al.*, 2002). In addition to these forward genetics approaches, reverse genetics is being used to study the large families of predicted glycosyl transferases and enzymes involved in the synthesis of

nucleotide sugars present in the *Arabidopsis* genome (Richmond and Somerville, 2000; Sarria *et al.*, 2001). With the tools available in *Arabidopsis*, mutants can be generated relatively easily. However, a major bottleneck in these functional genomics approaches is the characterization of the cell wall changes in the mutants. Chemical analysis of cell wall polysaccharides requires the homogenization of tissues leading to the loss of tissue- and cell-type-specific information. In addition, the amount of plant material available, especially for embryo-lethal mutants, precludes detailed cell wall analyses. Antibodies against specific sugar epitopes provide information on the distribution of polysaccharides within tissues, but this approach also has its pitfalls (Willats *et al.*, 2001). Micro-spectroscopic methods potentially provide a valuable alternative (Bonetta *et al.*, 2002; McCann *et al.*, 1997). Fourier-Transform Infrared (FT-IR) microspectroscopy is currently the most promising technique. With this technique, *Arabidopsis* and flax mutants with altered cell walls could be distinguished from wild-type controls (Chen *et al.*, 1998). FT-IR spectra from cell wall preparations provide extremely complex pictures of the total mixture of chemical bonds, and a major challenge is to correlate changes in the spectra with changes in cell wall composition or architecture (Wilson *et al.*, 2000). Purified polymers can be identified based on spectral data (Kacurakova *et al.*, 2000 and references therein), but the interpretation of complex mixtures of polysaccharides is currently practically impossible because of overlapping absorption maxima and spectral frequency shifts caused by interactions between molecules. Another complication is that FT-IR spectra are sensitive to variation among biological samples. Comparison between spectra needs to compensate for this variation in order to extract consistent differences linked to experimental treatments or genetic backgrounds. Digital subtraction of average spectra can provide information (McCann *et al.*, 1997), but does not take into account this variation. Another, frequently used strategy is to apply Principle Component Analysis (PCA) (Kemsley, 1998) as a data compression technique and to compare the loadings of discriminating PCs with spectra of purified polymers (Fagard *et al.*, 2000; Schindelman *et al.*, 2001; Sorensen *et al.*, 2000). As shown in this report, however, this approach does not always give unambiguous results. Here, we present an alternative procedure to circumvent these problems. The principle behind this approach, which has been successfully applied to the classification and identification of bacterial (Helm *et al.*, 1991) and fungal isolates (Tintelnot *et al.*, 2000), is that information can be obtained on the chemical changes in unknown samples from their clustering with samples with known changes. To test the feasibility of the approach, we carried out an analysis of 51 *Arabidopsis* samples corresponding to known cell wall mutants, wild-type seedlings treated with chemicals, and a set of so far uncharacterized mutants. Experimental variation between measurements was dealt with by sampling hypocotyls grown in the dark, an easily reproducible environmental condition, and the use of a balanced sampling protocol. An unsupervised method for the selection of discriminant wave numbers from the spectra was developed, which allowed the calculation of the Mahalanobis distance between mutants and their hierarchical clustering. The identification of a cluster of cellulose-deficient mutants allowed the identification of wave numbers in the spectra that are diagnostic for walls with altered cellulose content.

Results

Spectra from dark-grown hypocotyls distinguish mutants from the wild type

Fifty-one lines were analyzed, corresponding to 46 mutants and the wild type treated or not, respectively, with the microtubule-depolymerizing drug oryzaline or the cellulose synthesis inhibitors 2-6-dichlorobenyonitrile (DCB) or isoxaben. The phenotypic characteristics of the mutants and, if known, the nature of the genetic lesions are summarized in Table 1. Figure 1 shows an overview of the phenotypes of 4-day-old dark-grown seedlings. The reference mutants, which display a wide array of cell wall defects, frequently showed altered hypocotyl growth.

FT-IR spectra in transmission mode were collected from a 50 μm $\times$ 50 μm window halfway the hypocotyl of 4-day-old dark-grown seedlings while avoiding the central cylinder. Hypocotyls have a very simple anatomy (Gendreau *et al.*, 1997), and spectra correspond to the absorbance of only two epidermal and four cortical cell layers. Representative baseline-corrected and area-normalized spectra of the wild type Col-0 and dwarf mutants, respectively, with a cellulose deficiency (Fagard *et al.*, 2000) and reduced galacturonic acid content (Bouton *et al.*, 2002) are shown in Figure 2. We selected a window between 802 and 1820 cm^{-1}, represented by 265 data points, which contains information characteristic for polysaccharides. Besides a few frequencies clearly resolved in the spectrum, like the band at 1740 cm^{-1} corresponding to carboxylic esters (Kacurakova *et al.*, 2002), most of the spectrum was too complex to be interpreted visually. To obtain information on the spectral differences between the wild type and mutants, a digital subtraction of the spectra was attempted. Surprisingly, despite the different cell wall defects in the two mutants, the difference spectra were very comparable, with peaks covering most of the spectrum. These global differences did not allow an easy interpretation of the chemical nature of the cell wall defects in both types of mutants. We next carried out an exploratory PCA, which is a technique frequently used to distinguish groups of spectra (Chen *et al.*,

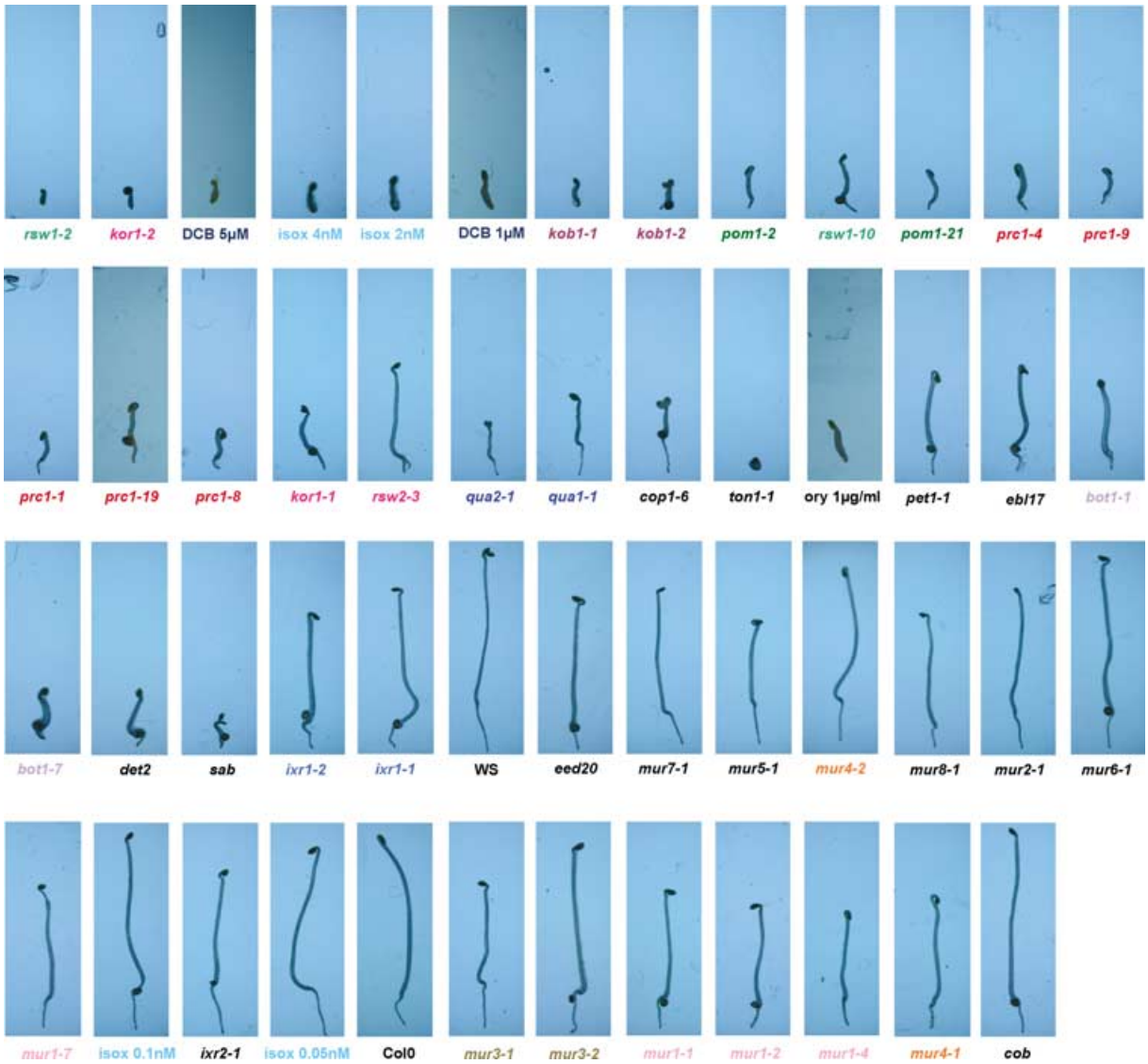

Figure 1. Phenotypes of 4-day-old dark-grown seedlings used in this study.
Mutants are described in Table 1. The order of the mutants is as in Figure 4. The height of each rectangle is 1.8 cm.

1998; Kemsley, 1998). Binary comparisons between mutant and the wild type identified in each case one major PC (Figure 3), which explained 90% of the variance and which clearly separated mutant from wild-type spectra. The PC1 loading for the comparison between the wild type and *prc1-8* resembled the difference spectrum with peaks at frequencies characteristic for not only cellulose but also other polysaccharides and protein (Fagard *et al.*, 2000). As for the difference spectra, the PC1 loading of the comparison between the wild type and *qua1-1* was also very similar to that of the wild type/*prc1-1* comparison. This suggests that, in both cases, the major PC used information from the entire spectrum, which appeared to mask information related to biologically relevant differences in cell wall composition. In conclusion, PCA allowed a distinction between the wild type and cell wall mutants, but did not provide clear-cut information on the exact nature of the cell wall changes.

Classification of FT-IR spectra

We next investigated whether a classification procedure could provide more information on the chemical differences between the mutants. To carry out such a classification, we chose to calculate the Mahalanobis distance among the *Arabidopsis* lines. The interest of the Mahalanobis distance is that it reduces the redundancy caused by the large number of correlated frequencies in the spectra. This calculation requires the inverse of the covariance matrix between the frequencies. However, this inverse matrix cannot be calculated as long as the number of

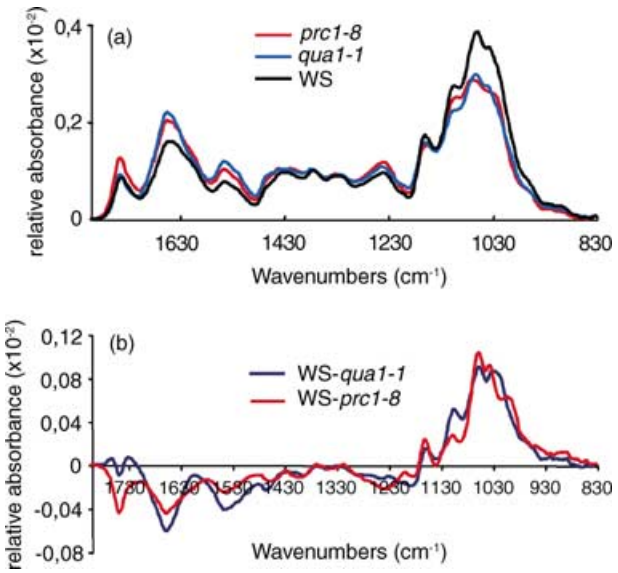

Figure 2. Cellulose-deficient mutant (*prc1-8*) and pectin-deficient mutant (*qua1-1*) show similar difference spectra with the wild type (WS).
(a) Average Fourier-Transform Infrared (FT-IR) spectra.
(b) Difference spectra obtained by digital subtraction from the WS average spectrum, respectively, of the *qua1-1* and *prc1-8* average spectrum.

variables exceeds the number of average spectra. As a result, a data compression technique was needed. The most straightforward technique is the Discriminant Variables Selection (DVS) method, which aims at selecting the subset of the most discriminating variables. This method is based on a stepwise algorithm that enters at each step the variable that gives the best improvement in mutant discrimination. This improvement is measured according to a Fisher ratio test, and the algorithm stops as soon as this test becomes non-significant. The DVS algorithm led to the selection of 39 wave numbers, which are shown plotted onto the average spectrum in Figure 4. Selected wave numbers covered the entire spectrum. Interestingly, many selected wave numbers corresponded to peaks or shoulders in the spectrum. Some areas, such as the area around 1630 cm^{-1}, were excluded, despite the presence of prominent and highly variable peaks. These peaks were not discriminant because of the large variance caused by experimental conditions. Based on the Mahalanobis distances calculated using the 39 selected wave numbers, a dendrogram was constructed using the Ward clustering algorithm (Anderberg, 1973).

Biological validation of the classification: all cellulose-deficient mutants were clustered

The dendrogram showed two main branches (Figure 4). Among the mutants within the upper branch, previous studies had demonstrated reduced cellulose content in the walls of *prc1* (Fagard *et al.*, 2000), *kob1* (Pagant *et al.*, 2002), *rsw2* (Lane *et al.*, 2001) and *rsw1* (Arioli *et al.*, 1998) alleles. The same branch also contained wild-type

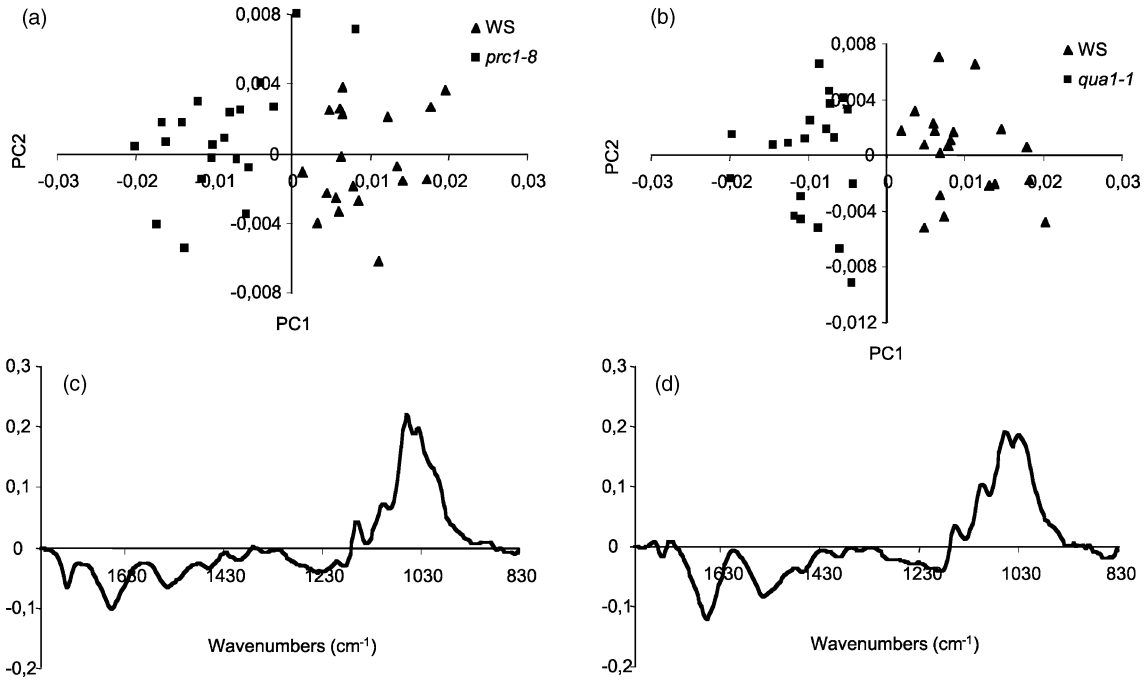

Figure 3. Exploratory Principle Component Analysis (covariance matrix) separates the wild type (WS) from mutant (*prc1-8* and *qua1-1*) spectra.
(a, b) A plot of the first two PCs shows that mutant and wild-type spectra can be separated by the first PC score.
(c, d) Loadings for PC1 contains information covering the entire spectrum. Note the similarity between the loadings despite the very different cell wall defects in the mutants (cellulose-deficiency in *prc1-8* and reduced pectin content in *qua1-1*).

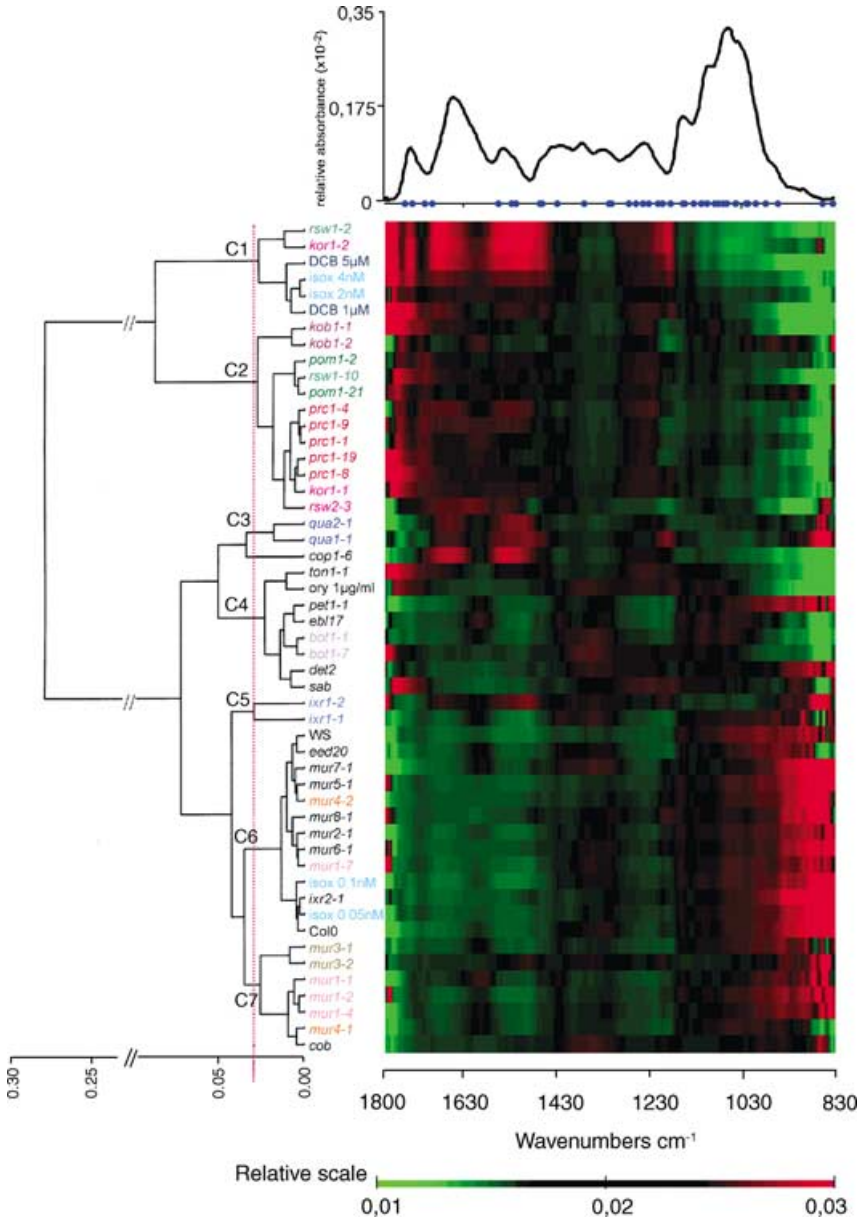

Figure 4. Dendrogram obtained by hierarchical cluster analysis of *Arabidopsis* lines based on their FT-IR spectra.
Alleles for the same gene have the same color. Semi/partial *R*/squared values are shown on the *x*-axis. Mutants are as in Table 1. C1–C7 are the clusters discussed in the text. Cluster analysis was carried out using the Ward clustering algorithm. Note that most alleles are clustered as well as all cellulose-deficient lines (C1 and C2). At the right side of the figure, the absorbance value for each wave number divided by the sum of the column of all values for that wave number is shown using the color code shown at the bottom of the figure. An average spectrum for the wild type Col-0 is shown at the top of the figure; the 39 selected variables are shown as blue dots.

seedlings treated, respectively, with the cellulose synthesis inhibitors DCB (1 and 5 µM) and isoxaben (2 and 4 nM). *Kor1-1*, which is allelic to *rsw2*, also showed a reduced cellulose synthesis as shown by the reduced incorporation of ^{14}C-Glc into the acetic/nitric acid-resistant cellulosic wall fraction (Figure 5). So, despite the entirely unsupervised nature of the classification procedure, it led to the clustering of all the reference lines for which reduced cellulose content had been reported. Interestingly, the upper branch also contained the two *pom1* alleles. *pom1* was previously described as a Conditional Root Expansion (CORE) mutant (Hauser *et al.*, 1995), *POM1* is identical to *ECTOPIC DEPOSITION OF LIGNIN IN PITH, ELP1* (Marie-Theres Hauser, personal communication), which encodes a putative secreted protein of the basic chitinase family (Zhong *et al.*, 2002). To test the prediction from the model, cellulose synthesis in 4-day-old dark-grown seedlings was compared between *pom1-21* and the wild type. The mutant indeed showed dramatically reduced cellulose synthesis compared to the wild type (Figure 5). For comparison, among the short hypocotyl mutants within the lower main branch, no defect in the synthesis of cellulose was observed for *bot1* and an over twofold increase for *qua1-1* and *qua2-1.* The upper branch was split into two subbranches, referred to as cluster 1 and 2 in Figure 4. Cluster 1 contained the more severely dwarfed alleles *rsw1-2* (Gillmor *et al.*, 2002) and

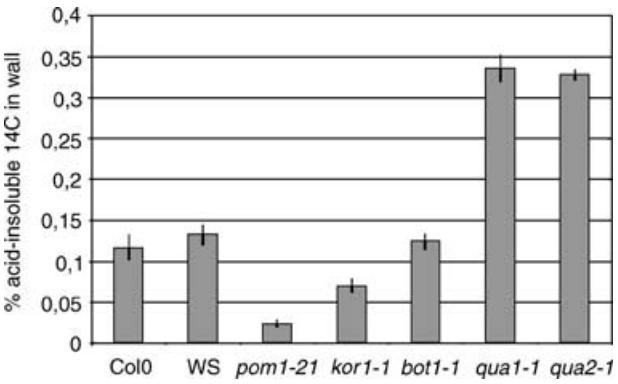

Figure 5. Relative cellulose synthesis activity in mutants.
Incorporation of ^{14}C-Glc in acid-resistant cellulosic material expressed as percentage of incorporation in the total cell wall. *pom1* and *kor1-1* show a reduced relative incorporation of ^{14}C-Glc in the cellulosic fraction compared to the wild type, whereas equally dwarfed mutants showed no difference (*bot1-1*) or an over twofold increase (*qua1-1* and *qua2-1*) in this incorporation compared to the wild type.

kor1-2 (Zuo *et al.*, 2000) and the wild type treated with the herbicides, whereas most mutants within cluster 2 showed weaker growth defects (Figure 1).

Biological validation of the classification: alleles of comparable strength are clustered

The sensitivity of the classification procedure was further demonstrated by the observation that almost all alleles of mutants corresponding to a wide variety of genetic lesions were grouped together. This was shown for the mutants with cellulose defects (five *prc1* alleles, two *pom1* alleles, and two *kob1* alleles), mutants with altered xyloglucan structure (two *mur3* alleles), mutants with reduced L-fucose content in cell walls (three *mur1* alleles), and even mutants with altered orientation of cortical microtubules (two *bot1* alleles) (Figure 4; Table 1). However, some lines did not cluster with their alleles. This was observed for *rsw1-2*, which did not cluster with *rsw1-2* and the three *kor* alleles *kor1-2*, *kor1-1*, and *rsw2-3*. In addition, *mur1-7* and *mur4-2* did not cluster, respectively, with the three other *mur1* alleles and *mur4-1*. Interestingly, in all these cases, the allele strength differed significantly, as shown by the much shorter hypocotyl for *rsw1-10* and *kor1-2* compared to that for *rsw1-10*, *kor1-1*, and *rsw2-3* (Figure 1), as well as the less severe reduction in L-fucose or L-arabinose content previously reported, respectively, for *mur1-7* and *mur4-2* compared to the other *mur1* and *mur4* alleles (Table 1). Interestingly, *mur1-7* and *mur4-2* were present in a cluster that also contained the wild type controls, suggesting that their phenotypes were more similar to the wild type than those of the stronger alleles. The clustering of the alleles of comparable strength among the 51 samples indicates that the spectra contained information specifically related to the phenotype of a wide range of cell wall and cytoskeleton mutants, and that the clustering procedure was able to extract this information.

Interpretation of other clusters

The lower branch contained a large cluster (cluster 6 in Figure 4), which contained the two wild-type accessions Col-0 and WS together with Col-0 treated with suboptimal concentrations of isoxaben, as well as a number of mutants. The proximity of all these samples to the wild type suggested that the mutations or treatments only influenced the IR phenotype marginally if at all. Among these mutants, *mur2-1* is best characterized (Reiter *et al.*, 1997; Vanzin *et al.*, 2002). The lack of L-fucose in *mur2-1* xyloglucan also has been confirmed in dark-grown seedlings (Lerouxel *et al.*, 2002). This small structural change, apparently, did not cause major changes in the FT-IR spectra. However, differences may become visible by including other *mur2* alleles in the analysis, which should improve the signal to noise ratio. It is interesting that, in contrast to *mur2*, both alleles of *mur3*, which not only lack L-Fuc but also L-Gal on the fourth position of the xyloglucan repeat units (Lerouxel *et al.*, 2002), were clearly separated from cluster 6. This much larger spectral difference suggests that a major change had occurred in the cell wall architecture caused by the further removal of the Gal residue from the XG. It is also intriguing that *mur4-1*, which has a reduced L-Ara content, clustered with *mur1* alleles. The reduced L-Fuc content in *mur1* not only affects XG, but also AGPs and RG2. O'Neill *et al.* (2001) recently showed that the absence of L-Fuc on RG2 interferes with its ability to form boron-diester-linked dimers. Interestingly, addition of excess boron not only restored dimer formation but also reverted the growth phenotype of the mutant. RG2 also contains L-Ara, and it is, therefore, not excluded that dimer formation is also affected in *mur4*. A common defect in RG2 may explain the similarity of the IR phenotype of *mur1* to that of *mur4-1*. Although *mur4-1* did not show a growth phenotype, the strongly additive effects of *mur4-1* with *mur1-1* in double mutant combinations (Burget and Reiter, 1999) are consistent with an effect of both mutations on RG2 dimer formation. The two *bot1* mutants, despite the absence of chemically observable cell wall defects (Figure 5; H.H., unpublished data), also formed a distinct group. The FT-IR spectra may therefore contain cytoplasmic information, information related to the different cell geometry, and/or information related to the altered orientation of microfibrils observed in this mutant (Burk *et al.*, 2001; Wasteneys and H.H., unpublished data). Interestingly, *bot1* clustered with the microtubule mutant *ton1* and the wild type treated with the inhibitor of microtubule polymerization oryzaline. It will be interesting to see whether the other mutants in cluster 4, *pet1-1, ebl17*, *det2*, and *sab*, also have altered microtubule organization. Cluster 3

contained *qua1-1* and *qua2-1*, both of which are putative pectin mutants (Bouton, 2001; Bouton *et al.*, 2002). Finally, *ixr1-2* and *ixr1-1* formed a cluster distinct from the wild type, suggesting that, besides the isoxaben resistance, the mutations have other phenotypic effects.

Interpretation of the spectral differences between mutants and the wild type

Figure 4 shows that, in addition to the selected most discriminant frequencies, large parts of the spectra varied between the lines and the clustering procedure indeed seemed to have grouped lines with related spectra. Given the large cluster of cellulose-deficient mutants, we investigated whether this cluster could be used to identify diagnostic wave numbers for altered cellulose content in the context of an intact cell wall. To this end, we compared the average spectrum from cluster 1 and cluster 2 with that of cluster 6, which contained the wild-type lines WS and Col-0. A Student's *t*-test was used to determine the significance of the difference between average values for every individual wave number of the spectrum. The significance value or *t*-value was plotted against the wave numbers of the spectrum (Figure 6). Interestingly, among the highly significant positive *t*-values (higher in the wild type than in cellulose-deficient cluster), a series of prominent peaks could be seen at wave numbers that previously had been assigned to various linkages of the β-1,4-glucan polymer. Indeed, 1369 and 1319 cm^{-1} had been assigned to a CH_2 stretch of cellulose (Kacurakova *et al.*, 2002), 1157 cm^{-1} to the glycosidic C–O–C vibration of cellulose (Kacurakova *et al.*, 2000), the doublet at 1060 and 1037 cm^{-1} to the C–O–C and C–C bonds of the cellulose sugar rings (Kacurakova *et al.*, 2000), 990 cm^{-1} to a bond shared by cello-triose, -tetraose and -pentose (Sekkal *et al.*, 1995) and the smaller 898 cm^{-1} peak to the β-anomeric bond of cellulose (Kacurakova *et al.*, 2000). Together, all these wave numbers are consistent with a reduced cellulose content in the samples of cluster 1 and 2. Interestingly, some discriminant wave numbers (e.g. 1157 cm^{-1}) corresponded to peaks in the spectrum (compare Figure 6a,b), whereas others, such as 990 cm^{-1}, did not correspond to discernable peaks. This nicely illustrates that very subtle spectral changes can be highly significant and diagnostic for defined changes in polymer composition. Figure 6(b) also shows strong negative and sharp peaks at 1762, 1735, and 1712 cm^{-1}, which correspond to carboxylic ester linkages presumably of esterified pectins (Sene *et al.*, 1994). The negative peak at 1245 cm^{-1} had been assigned previously to C–O vibrations in pectic polysaccharides (Kacurakova *et al.*, 2002). The nature of the negative peaks at 1442 and 1631 cm^{-1} and some other positive peaks remains to be determined. Together, these results convincingly demonstrate that the cell walls of the mutants of cluster 1 and 2 contained less cellulose and more esterified pectic polysaccharides. The multiple wave numbers corresponding to the ester bonds suggest that distinct carboxylic ester linkages had appeared in the mutants, or that the reduced cellulose content had caused changes in the chemical environment of subsets of pectic polysaccharides.

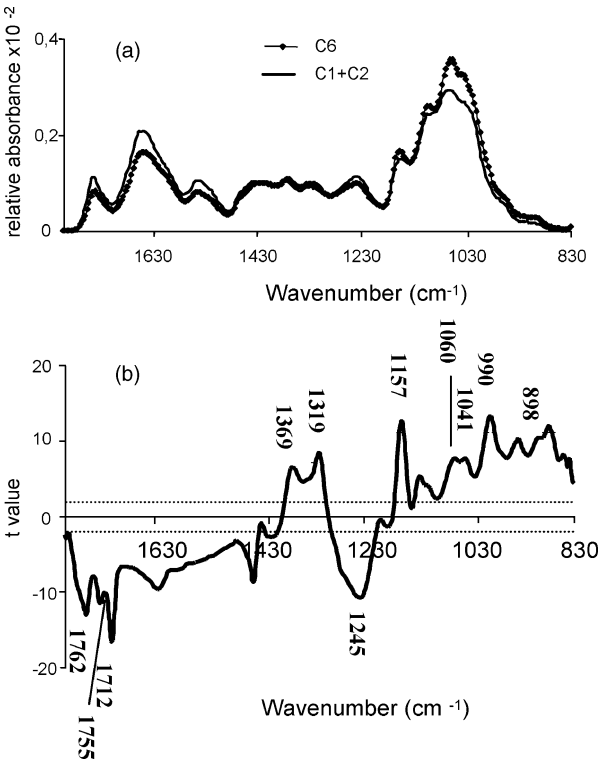

Figure 6. Reduced cellulose content and increased esterified pectin content are observed in cluster 1 and 2 compared to the wild-type-containing cluster 6. Wave numbers for which absorbance values are significantly different between cluster 1 + 2 (cellulose-deficient lines) and cluster 6 (lines similar to the wild types) were identified using a Student's *t*-test.
(a) Average spectra for cluster 1 + 2 and cluster 6.
(b) Student's *t*-test: *t*-value for the comparison between cluster 1 + 2 and cluster 6 (*y*-axis) is plotted against the wave numbers (*x*-axis). Horizontal lines refer to the $P = 0.95$ significance threshold. Several highly significant maxima (1369, 1319, 1157, 1060, 1041, 990, and 898 cm^{-1}) could be assigned to linkages in the cellulose polymer (see text). Equally significant minima could be assigned to ester linkages (1762, 1735, and 1712 cm^{-1}) and C–O vibrations of pectin (1245 cm^{-1}).

Discussion

The results described in this paper demonstrate that FT-IR microspectroscopy can be used not only to distinguish *Arabidopsis* mutants from the wild type but also to classify different types of cell wall and cytoskeleton mutants. The power of this approach is its completely unsupervised nature: the only request to the algorithm was to calculate distances between the 51 lines. The clustering of alleles illustrated the sensitivity of the procedure to extract biologically relevant information associated with a wide variety

of cellular defects (cellulose deficiency, alterations in xyloglucans, pectin and other cell wall polysaccharides, and altered cortical microtubules) from complex spectra sampled from intact seedlings. Interestingly, FT-IR allowed a more refined distinction between cellulose-deficient mutants than chemical analysis alone. Indeed, within the large cellulose-deficient cluster, mutants that were chemically and morphologically indistinguishable could be distinguished based on their spectra. The presence of *pom1* in a cluster with exclusively cellulose-deficient lines led to the prediction that this mutant is also cellulose deficient, which was confirmed chemically. The exact role of the basic chitinase-like POM1 protein in the synthesis of cellulose remains to be determined, but these findings add a new essential element to the cellulose synthesis machinery in plants.

The identification of clusters provided a powerful way to identify those wave numbers in the spectrum that most reliably distinguish groups of mutants with comparable defects from the wild type. This was illustrated for the cluster of cellulose-deficient lines. A set of wave numbers was identified that showed highly significant differences in absorbance values between the clusters containing the cellulose-deficient lines and a reference cluster containing the two wild-type lines. Interestingly, the majority of the wave numbers could be interpreted and were entirely consistent with a reduced cellulose content and an increased level of esterified pectins in the mutants. The results confirm previous observations (His *et al.*, 2001; Peng *et al.*, 2000) that important, presumably compensatory, changes in the pectin composition occurred in the wall of cells in which cellulose synthesis was inhibited. Some frequencies, however, could not be assigned to known sugar linkages and may be related to other architectural changes induced by a reduced cellulose content. These wave numbers can now be used to follow cellulose content in different developmental contexts such as in growth, cell division or differentiation gradients in growing organs, or in different environmental conditions. With the availability of a larger pool of reference mutants, it also may become possible to identify diagnostic wave numbers for other polysaccharides within the context of an intact cell wall. In addition to the hypocotyl, other organs and cell types can be targeted such as the xylem cells on transverse sections of inflorescence stems (G. Mouille and L. Jouanin, unpublished data). The technique is simple and rapid and, combined with reverse genetics, represents a valuable addition to the plant functional genomics toolbox.

Experimental procedures

Plant material and growth conditions

Arabidopsis wild types and mutants are summarized in Table 1. Lines obtained from the *Arabidopsis* Biological Resource Center, Ohio or the Nottingham *Arabidopsis* Stock Center were first amplified in the greenhouse. Novel lines were obtained from a screen of T-DNA mutagenized T2 or T3 families. Seeds were plated on a medium (Estelle and Somerville, 1987) without sucrose, kept for 2 days at 4°C, and exposed to continuous white light (200 μmol m^{-2} sec^{-1}) for 4 h prior to incubation in the dark (Petri dishes wrapped in three layers of aluminum foil) for 4 days in a growth chamber at 20°C with 70% relative humidity. Stock solutions of inhibitors DCB and isoxaben (kindly provided by Pierre Leroux, INRA, Versailles) and oryzalin (kindly provided by Jan Traas, INRA, Versailles) were made in dimethyl sulfoxide (DMSO). The generation of T-DNA lines was described by Bechtold and Pelletier (1998).

Sampling of FT-IR spectra

Four-day-old seedlings were squashed between two BaF_2 windows and abundantly rinsed in distilled water for 2 min. The samples were then dried on the window at 37°C for 20 min. An area of 50 μm × 50 μm halfway the hypocotyl, on the side of the central cylinder, was selected for spectra collection. Spectra were collected using a ThermoNicolet Nexus spectrometer with a Continuum microscope accessory. Fifty interferograms were collected in transmission mode with 8 cm^{-1} resolution and co-added to improve the signal-to-noise ratio of the spectrum.

Statistical analysis

The exploratory Principal Component Analysis was carried out by using WIN-DISCRIM software (E.K. Kemsley, Institute of Food Research, Norwich, UK).

Further and more detailed statistical analysis was carried out with the SAS software V8.0 (SAS Institute, 1999). SAS codes are available upon request to the corresponding author. For a detailed description of the statistical analysis, see Robin *et al.* (2003).

Data set and normalization

For each of the $M = 51$ lines, plants were grown in $D = 4$ different Petri dishes and $R = 5$ seedlings were sampled in each dish. The total data set consists of $M \times D \times R = 1020$ spectra. Denoting $X(n)$ the absorbance for the wave number n ($n = 1,\ldots,N$), the spectrum of the plant r in dish d of mutant m is $Xmdr = [Xmdr(1) \ldots Xmdr(N)]$. To normalize the spectra, the baseline was estimated using a linear regression involving 10 points at each end of the spectrum and then subtracted from each absorbance value. The area under each spectrum was set to one by dividing each absorbance by the sum of all absorbances. Normalizations were carried out with the Octave package (Eaton, 1999).

Calculation of the Mahalanobis distance between mutants

The Mahalanobis distance between lines was calculated. Denote Σ as the $N \times N$ covariance matrix between wave numbers for each mutant (N being the number of wave numbers: $n = 1, \ldots, N$). This matrix is assumed to be the same for all mutants. $X(m)$ denotes the mean spectrum of mutant number m; the row vector with N coordinates $X(m, n)$ is the mean absorbance of mutant m for wave number n. The (squared) Mahalanobis distance between mutants m and m' is the distance between vector $X(m)$ and $X(m')$ using the inverse of Σ a metric (Arnold, 1981).

Table 1 Overview of the mutants used in this study

Mutant	Phenotype	Mutated gene product	Ecotype	Reference
bot1-1	Dwarf, disorganized cortical interphase microtubules, reduced anisotropic expansion	P60 subunit of microtubule severing katanin AtKTN1. Most likely null mutation	Col-0	(Bichet *et al.*, 2001; Burk *et al.*, 2001)
bot1-7	Idem	Idem	WS	Idem
cob	Increased radial expansion in root	GPI-anchored protein	Col-0	(Benfey *et al.*, 1993; Schindelman *et al.*, 2001)
cop1-6	Constitutive photomorphogenic development in the dark	E3 ubiquitin ligase involved in light-regulated degradation of transcription factors	Col-0	(Deng *et al.*, 1991; Quail, 2002)
det2	De-etiolated dark grown seedling. Brassinosteroid sensitive dwarf	Steroid 5α-reductase in brassinolide biosynthetic pathway	Col-0	(Li et al., 1996)
ebl17	Short hypocotyl in dark-grown seedlings	Unknown	Col-0	(Höfte H., unpublished data)
eed20	Short hypocotyl in dark-grown seedlings	Unknown	WS	(Höfte H., unpublished data)
ixr1-1	Semi-dominant mutation conferring increased resistance to isoxaben	Cellulose synthase catalytic subunit CESA3	Col-0	(Scheible *et al.*, 2001)
ixr1-2	Idem	Idem	Idem	Idem
ixr2-1	Semidominant mutation conferring increased resistance to isoxaben	Cellulose synthase catalytic subunit CESA6	Col-0	(Desprez *et al.*, 2002)
kob1-1	Dwarf, cellulose deficiency	Novel intrinsic plasma membrane protein, most likely null mutation	WS	(Pagant *et al.*, 2002)
kob1-2	Idem	Idem	Col-0	Idem
kor1-1	Dwarf, cellulose deficiency, increased pectin content	Membrane-bound endo-β-1,4-glucanase	WS	(Lane *et al.*, 2001; Nicol *et al.*, 1998)
kor1-2	Seedling lethal	Idem	Col-0	(Zuo *et al.*, 2000)
mur1-1	L-fucose content in aerial organs reduced to 1% of the wild type. Replacement of L-fucose by L-galactose in xyloglucans. Reduced dimerization of RG-II	GDP-D-mannose-4,6-dehydratase	Col-0	(Bonin *et al.*, 1997; Zablackis *et al.*, 1996)
mur1-2	Idem	Idem	Idem	Idem
mur1-4	Idem	Idem	Idem	Idem
mur1-7	L-fucose content in aerial organs reduced to 10% of the wild type.	Idem	Idem	Idem
mur2-1	L-fucose content in organs reduced to 50% of the wild type	Xyloglucan-fucosyl transferase	Idem	(Reiter *et al.*, 1997; Vanzin *et al.*, 2002)
mur3-1	L-fucose content in aerial organs reduced to 50% of the wild type	Xyloglucan-galactosyl transferase	Idem	(Lerouxel *et al.*, 2002; Reiter *et al.*, 1997)
mur3-2	Idem	Idem	Idem	Idem
mur4-1	L-arabinose content in aerial organs reduced to 50% of the wild type. Reduced membrane-bound UDP-xylose 4-epimerase activity	Unknown	Idem	(Burget and Reiter, 1999; Reiter *et al.*, 1997)
mur4-2	L-arabinose content in aerial organs reduced to 75% of the wild type.	Idem	Idem	Idem
mur5-1	L-arabinose content in aerial organs reduced to 70% of the wild type	Unknown	Idem	(Reiter *et al.*, 1997)
mur6-1	L-arabinose content in aerial organs reduced to 70% of the wild type	Unknown	Idem	Idem
mur7-1	L-arabinose content in aerial organs reduced to 70% of the wild type	Unknown	Idem	Idem
mur8-1	L-rhamnose content in aerial organs reduced to 65% of the wild type	Unknown	Idem	Idem
pet1-1	Sucrose-dependent short hypocotyl phenotype, shortened cells	Unknown	Idem	(Kurata and Yamamoto, 1998)
pom1-2	Abnormal cell expansion in root, ectopic deposition of lignin	Basic chitinase-like protein	Col-0	(Zhong *et al.*, 2002; Hauser M.T., personal communication)

Table 1 continued

Mutant	Phenotype	Mutated gene product	Ecotype	Reference
pom1-21	Idem	Idem	WS	Idem
prc1-1	Short hypocotyl in dark-grown seedlings, short root, cellulose deficiency	Cellulose synthase catalytic subunit gene CESA6, most likely null mutation	Col-0	(Desnos *et al.*, 1996; Fagard *et al.*, 2000)
prc1-4	Idem	Idem	Idem	Idem
prc1-8	Idem	Idem	Idem	Idem
prc1-9	Idem	Idem	Idem	Idem
prc1-19	Idem	Idem	Idem	Idem
qua1-1	Dwarf, reduced cell adhesion, galacturonic acid content reduced to 75% of the wild type	Putative membrane bound family 8 glycosyltransferase	WS	(Bouton *et al.*, 2002)
qua2-1	Idem	Unknown	Col-0	(Bouton, 2001)
rsw1–2	Seedling lethal, increased radial expansion and cellulose deficiency	Cellulose synthase catalytic subunit CESA1	Col-0	(Gillmor *et al.*, 2002)
rsw1–10	Root swelling, dwarf cellulose deficiency	Idem	WS	(Arioli *et al.*, 1998; Baskin *et al.*, 1995; Fagard *et al.*, 2000)
rsw2–3^{ts}	Cellulose deficiency, increased pectin content	Membrane-bound endo-β-1,4-glucanase	Col-0	(Lane *et al.*, 2001)
sab	Dwarf, increased radial cell expansion	Novel large protein	WS	(Aeschbacher *et al.*, 1995)
ton1–1	Defect in organization of cortical microtubules	Novel protein (D. Bouchez, personal communication)	Col-0	(Traas *et al.*, 1995)

Data compression

The calculation of the Mahalanobis requires the inversion of the (estimated) matrix Σ. This matrix is not invertible if the number of frequencies N is higher than $M(R-1)$. The dimension of the data set, therefore, needs to be reduced using a compression technique. In this report, we used the DVS (SAS procedure: stepdisc with slentry $= 10^{-3}$, slstay $= 10^{-3}$ options), which aims at selecting the most discriminant wave numbers between mutants. The selection criterion was the Fisher ratio associated with the mutant effect in an analysis of covariance (ANCOVA) model where variables already selected are used as co-variates (Hand, 1981). The same kind of ANCOVA model was used to remove variables from the selection. This led to a stepwise procedure. In our studies, we used the same level for entering and removing variables.

Mutant clustering

Once the Mahalanobis distances between mutants were calculated (SAS procedure: discrim), we used the Ward algorithm (SAS procedure: cluster) to define groups of similar mutants. At each step, the Ward algorithm chooses the two mutants to be grouped in such a way that the remaining variance of the data set remains maximal.

Cellulose synthesis assay

Quantification of cellulose synthesis activity using ^{14}C-Glc incorporation was performed as described by Fagard *et al.* (2000).

Acknowledgements

Wolf Dieter Reiter, the *Arabidopsis* Biological Research Center, Ohio and the Nottingham *Arabidopsis* Stock Center are thanked for providing mutants, and Marie-Theres Hauser and Philip Benfey for *pom1* and *sab*. Sandra Pelletier and Estelle Aletti are thanked for skilful technical assistance, Bruno Letarnec for technical assistance in the greenhouse. Geoff Wasteneys is thanked for allowing us to cite his unpublished data, Hoai-Nam Truong and Sophie Bouton for *qua1* and *qua2*, and Marc Lahaye for sugar composition analysis in *qua1* and *qua2*. Dominique Bertrand is thanked for the critical reading of the manuscript and communicating his excellent insights in chemometrics. Joëlle Amselem is thanked for help with making Figure 5. Part of the work was funded by EEC Framework 5 projects EUROPECTIN and GEMINI, GENOPLANTE grants 1999025 and 2001035, and Ministry of Research and Technology and CIRAD PhD fellowships to S.P. and Action Concertée Incitative 2000 grant 47 to H.H.

References

Aeschbacher, R.A., Hauser, M.T., Feldmann, K.A. and Benfey, P.N. (1995) The SABRE gene is required for normal cell expansion in *Arabidopsis*. *Genes Dev.* **9**, 330–340.

Anderberg, H.H. (1973) *Cluster Analysis for Applications*. New York: Academic Press, Inc.

Arioli, T., Peng, L., Betzner, A.S. *et al.* (1998) Molecular analysis of cellulose biosynthesis in *Arabidopsis*. *Science*, **279**, 717–720.

Arnold, S.F. (1981) *The Theory of Linear Models and Multivariate Analysis*. New York: Wiley.

Baskin, T., Herth, W., Cork, A., Birch, R., Rolfe, B., Redmond, J. and Williamson, R. (1995) Radial swelling mutants deficient in cellulose biosynthesis. *J. Cell. Bioch. Abstract supplement*, **21A**, 440.

Bechtold, N. and Pelletier, G. (1998) *In planta Agrobacterium*-mediated transformation of adult *Arabidopsis thaliana* plants by vacuum infiltration. *Meth. Mol. Biol.* **82**, 259–266.

Benfey, P.N., Linstead, P.J., Roberts, K., Schiefelbein, J.W., Hauser, M.T. and Aeschbacher, R.A. (1993) Root development in *Arabidopsis* – four mutants with dramatically altered root morphogenesis. *Development*, **119**, 57–70.

Bichet, A., Desnos, T., Turner, S., GrandJean, O. and Höfte, H. (2001) BOTERO1 is required for normal orientation of cortical microtubules and anisotropic cell expansion in *Arabidopsis*. *Plant J.* **25**, 137–148.

Bonetta, D.T., Facette, M., Raab, T.K. and Somerville, C.R. (2002) Genetic dissection of plant cell-wall biosynthesis. *Biochem. Soc. Trans.* **30**, 298–301.

Bonin, C.P., Potter, I., Vanzin, G.F. and Reiter, W.D. (1997) The MUR1 gene of *Arabidopsis thaliana* encodes an isoform of GDP-D- mannose-4,6-dehydratase, catalyzing the first step in the *de novo* synthesis of GDP-L-fucose. *Proc. Natl. Acad. Sci. USA*, **94**, 2085–2090.

Bouton, S. (2001) Etude de la régulation transcriptionnelle de l'assimilation du nitrate chez Arabidopsis Thalina. Recherche de gènes régulateurs potentiels et caractérisation de mutants. PhD Thesis. University Paris XI, sciences de la vie.

Bouton, S., Leboeuf, E., Mouille, G., Leydecker, M.-T., Talbotec, J., Granier, F., Lahaye, M., Höfte, H. and Truong, H.N. (2002) QUASIMODO1 encodes a putative membrane-bound glycosyltransferase required for normal pectin synthesis and cell adhesion in *Arabidopsis*. *Plant Cell*, **14**, 2577–2590.

Burget, E.G. and Reiter, W.D. (1999) The *mur4* mutant of *Arabidopsis* is partially defective in the *de novo* synthesis of uridine diphospho L-arabinose. *Plant Physiol.* **121**, 383–389.

Burk, D.H., Liu, B., Zhong, R., Morrison, W.H. and Ye, Z.H. (2001) A katanin-like protein regulates normal cell wall biosynthesis and cell elongation. *Plant Cell*, **13**, 807–828.

Chen, L., Carpita, N.C., Reiter, W.D., Wilson, R.H., Jeffries, C. and McCann, M.C. (1998) A rapid method to screen for cell-wall mutants using discriminant analysis of Fourier-transform infrared spectra. *Plant J.* **16**, 385–392.

Deng, X.W., Caspar, T. and Quail, P.H. (1991) Cop1 – a regulatory locus involved in light-controlled development and gene expression in *Arabidopsis*. *Genes Dev.* **5**, 1172–1182.

Desnos, T., Orbovic, V., Bellini, C., Kronenberger, J., Caboche, M., Traas, J. and Hofte, H. (1996) Procuste1 mutants identify two distinct genetic pathways controlling hypocotyl cell elongation, respectively in dark- and light-grown *Arabidopsis* seedlings. *Development*, **122**, 683–693.

Desprez, T., Vernhettes, V., Fagard, S., Refregier, G., Desnos, T., Aletti, E., Py, N., Pelletier, S. and Höfte, H. (2002) Resistance against herbicide isoxaben and cellulose deficiency caused by distinct mutations in same cellulose synthase isoform CESA6. *Plant Physiol.* **128**, 482–490.

Eaton, E.A. (1999) *GNU Octave* Version 2.0.14. (http://www.octave.org).

Estelle, M.A. and Somerville, C.R. (1987) Auxin-resistant mutants of *Arabidopsis thaliana* with an altered morphology. *Mol. Gen. Genet.* **206**, 200–206.

Fagard, M., Desnos, T., Desprez, T., Goubet, F., Refregier, G., Mouille, G., McCann, M., Rayon, C., Vernhettes, S. and Höfte, H. (2000) PROCUSTE1 encodes a cellulose synthase required for normal cell elongation specifically in roots and dark-grown hypocotyls of *Arabidopsis*. *Plant Cell*, **12**, 2409–2423.

Gendreau, E., Traas, J., Desnos, T., Grandjean, O., Caboche, M. and Hofte, H. (1997) Cellular basis of hypocotyl growth in *Arabidopsis thaliana*. *Plant Physiol.* **114**, 295–305.

Gillmor, C.S., Poindexter, P., Lorieau, J., Palcic, M.M. and Somerville, C. (2002) a-Glucosidase I is required for cellulose biosynthesis and morphogenesis in *Arabidopsis*. *J. Cell. Biol.* **156**, 1003–1013.

Hand, D.J. (1981) *Discrimination and Classification*. New York: Wiley.

Hauser, M.T., Morikami, A. and Benfey, P.N. (1995) Conditional root expansion mutants of *Arabidopsis*. *Development*, **121**, 1237–1252.

Helm, D., Labischinski, H., Schallehn, G. and Naumann, D. (1991) Classification and identification of bacteria by Fourier-transform infrared spectroscopy. *J. Gen. Microbiol.* **137**, 69–79.

His, I., Driouich, A., Nicol, F., Jauneau, A. and Hofte, H. (2001) Altered pectin composition in primary cell walls of korrigan, a dwarf mutant of *Arabidopsis* deficient in a membrane-bound endo-β-1,4-glucanase. *Planta*, **212**, 348–358.

Kacurakova, M., Capek, P., Sasinkova, V., Weller, N. and Ebringerova, A. (2000) FT-IR study of plant cell wall model compounds: pectic polysaccharides and hemicelluloses. *Carbohydr. Polymers*, **43**, 195–203.

Kacurakova, M., Smith, A.C., Gidley, M.J. and Wilson, R.H. (2002) Molecular interaction in bacterial cellulose composites studied by 1D FT-IR and dynamic 2D FTIR spectroscopy. *Carbohydr. Res.* **337**, 1145–1153.

Kemsley, E.K. (1998) *Discriminant Analysis Of Spectroscopic Data*. Chichester, UK: John Wiley and Sons.

Kurata, T. and Yamamoto, K.T. (1998) *Petit1*, a conditional growth mutant of *Arabidopsis* defective in sucrose-dependent elongation growth. *Plant Physiol.* **118**, 793–801.

Lane, D.R., Wiedemeier, A., Peng, L. *et al.* (2001) Temperature-sensitive alleles of *rsw2* link the korrigan endo-β-1,4-glucanase to cellulose synthesis and cytokinesis in *Arabidopsis*. *Plant Physiol.* **126**, 278–288.

Lerouxel, O., Choo, T.S., Seveno, M., Usadel, B., Faye, L., Lerouge, P. and Pauly, P. (2002) Rapid structural phenotyping of plant cell wall mutants by enzymatic oligosaccharide fingerprinting. *Plant Physiol.* **130**, 1754–1763.

Li, J.M., Nagpal, P., Vitart, V., Mcmorris, T.C. and Chory, J. (1996) A role for brassinosteroids in light-dependent development of *Arabidopsis*. *Science*, **272**, 398–401.

Lukowitz, W., Nickle, T.C., Meinke, D.W., Last, R.L., Conklin, P.L. and Somerville, C.R. (2001) *Arabidopsis cyt1* mutants are deficient in a mannose-1-phosphate guanylyltransferase and point to a requirement of *N*-linked glycosylation for cellulose biosynthesis. *Proc. Natl. Acad. Sci. USA*, **98**, 2262–2267.

McCann, M.C., Chen, L., Roberts, K., Kemsley, E.K., Sene, S., Carpita, N.C., Stacey, N.J. and Wilson, R.H. (1997) Infrared microspectroscopy: sampling heterogeneity in plant cell wall composition and architecture. *Physiol. Plant.* **100**, 729–738.

Nicol, F., His, I., Jauneau, A., Vernhettes, S., Canut, H. and Hofte, H. (1998) A plasma membrane-bound putative endo-1,4-beta-D-glucanase is required for normal wall assembly and cell elongation in *Arabidopsis*. *EMBO J.* **17**, 5563–5576.

O'Neill, M.A., Eberhard, S., Albersheim, P. and Darvill, A.G. (2001) Requirement of borate cross-linking of cell wall rhamnogalacturonan II for *Arabidopsis* growth. *Science*, **294**, 846–849.

Pagant, S., Bichet, A., Sugimoto, K., Lerouxel, O., Desprez, T., McCann, M., Lerouge, P., Vernhettes, S. and Höfte, H. (2002) KOBITO1 encodes a novel plasma membrane protein necessary for normal cellulose synthesis during cell expansion in *Arabidopsis*. *Plant Cell*, **14**, 2001–2013.

Peng, L., Hocart, C.H., Redmond, J.W. and Williamson, R.E. (2000) Fractionation of carbohydrates in *Arabidopsis* root cell walls

shows that three radial swelling loci are specifically involved in cellulose production. *Planta*, **211**, 406–414.

Quail, P.H. (2002) Phytochrome photosensory signalling networks. *Nat. Rev. Mol. Cell Biol.* **3**, 85–93.

Reiter, W.D., Chapple, C. and Somerville, C.R. (1997) Mutants of *Arabidopsis thaliana* with altered cell wall polysaccharide composition. *Plant J.* **12**, 335–345.

Richmond, T.A. and Somerville, C.R. (2000) The cellulose synthase superfamily. *Plant Physiol.* **124**, 495–498.

Robin, S., Lecomte, M., Höfte, H. and Mouille, G. (2003) A procedure for the clustering of cell wall mutants in the model plant *Arabidopsis* based on Fourier transform infrared (FT-IR) spectroscopy. *J. Appl. Stat.* **30**, 669–681.

Sarria, R., Wagner, T.A., O'Neill, M.A., Faik, A., Wilkerson, C.G., Keegstra, K. and Raikhel, N.V. (2001) Characterization of a family of *Arabidopsis* genes related to xyloglucan fucosyltransferase1. *Plant Physiol.* **127**, 1595–1606.

SAS Institute (1999). *SAS/STAT User's Guide*. Cary: SAS Institute.

Scheible, W.R., Eshed, R., Richmond, T., Delmer, D. and Somerville, C. (2001) Modifications of cellulose synthase confer resistance to isoxaben and thiazolidinone herbicides in *Arabidopsis Ixr1* mutants. *Proc. Natl. Acad. Sci. USA*, **98**, 10079–10084.

Schindelman, G., Morikami, A., Jung, J., Baskin, T.I., Carpita, N.C., Derbyshire, P., McCann, M.C. and Benfey, P.N. (2001) COBRA encodes a putative GPI-anchored protein, which is polarly localized and necessary for oriented cell expansion in *Arabidopsis*. *Genes Dev.* **15**, 1115–1127.

Sekkal, M., Dincq, V., Legrand, P. and Huvenne, J.P. (1995) Investigation of the glycosidic linkages in several oligosaccharides using FT-IR and FT Raman spectroscopies. *J. Mol. Struct.* **349**, 349–352.

Sene, C., McCann, M.C., Wilson, R.H. and Grinter, R. (1994) Fourier-Transform Raman and Fourier-Transform Infrared Spectroscopy (An Investigation of Five Higher Plant Cell Walls and Their Components). *Plant Physiol.* **4**, 1623–1631.

Sorensen, O., Pauly, M., Bush, M., Skjot, M., McCann, M.C., Borkhardt, B. and Ulvskov, P. (2000) Pectin engineering: modification of potato pectin by *in vivo* expression of an endo-1,4-beta-D-galactanase. *Proc. Natl. Acad. Sci. USA*, **97**, 7639–7644.

Tintelnot, K., Haase, G., Seibold, M., Bergmann, F., Staemmler, M., Tatjana, F. and Naumann, D. (2000) Evaluation of phenotypic markers for selection and identification of *Candida dubliniensis*. *J. Clin. Microbiol.* **38**, 1599–1608.

Traas, J., Bellini, C., Nacry, P., Kronenberger, J., Bouchez, D. and Caboche, M. (1995) Normal differentiation patterns in plants lacking microtubular preprophase bands. *Nature*, **375**, 676–677.

Vanzin, G.F., Madson, M., Carpita, N.C., Raikhel, N.V., Keegstra, K. and Reiter, W.D. (2002) The *mur2* mutant of *Arabidopsis thaliana* lacks fucosylated xyloglucan because of a lesion in fucosyltransferase AtFUT1. *Proc. Natl. Acad. Sci. USA*, **99**, 3340–3345.

Willats, W.G., McCartney, L., Mackie, W. and Knox, J.P. (2001) Pectin: cell biology and prospects for functional analysis. *Plant Mol. Biol.* **47**, 9–27.

Williamson, R.E., Burn, J.E. and Hocart, C.H. (2001) Cellulose synthesis: mutational analysis and genomic perspectives using *Arabidopsis thaliana*. *Cell Mol. Life Sci.* **58**, 1475–1490.

Wilson, R.H., Smith, A.C., Kacurakova, M., Saunders, P.K., Wellner, N. and Waldron, K.W. (2000) The mechanical properties and molecular dynamics of plant cell wall polysaccharides studied by Fourier-transform infrared spectroscopy. *Plant Physiol.* **124**, 397–405.

Zablackis, E., York, W.S., Pauly, M., Hantus, S., Reiter, W.D., Chapple, C.C.S., Albersheim, P. and Darvill, A. (1996) Substitution of L-fucose by L-galactose in cell walls of *Arabidopsis mur1*. *Science*, **272**, 1808–1810.

Zhong, R., Kays, S.J., Schroeder, B.P. and Ye, Z.H. (2002) Mutation of a chitinase-like gene causes ectopic deposition of lignin, aberrant cell shapes, and overproduction of ethylene. *The Plant Cell*, **14**, 165–179.

Zuo, J., Niu, Q.W., Nishizawa, N., Wu, Y., Kost, B. and Chua, N.H. (2000) KORRIGAN, an *Arabidopsis* endo-1,4-beta-glucanase, localizes to the cell plate by polarized targeting and is essential for cytokinesis. *Plant Cell*, **12**, 1137–1152.